PAPER

A Dual-Band Decoupling Method of 2 Elements MIMO Antennas by Using a Short Stub and a Branch Element

Takuya MIYASAKA[†], **Hiroshi SATO**[††], ***Members***, ***and*** **Masaharu TAKAHASHI**[†a)], ***Fellow***

SUMMARY In recent years, MIMO technology which uses multiple antennas has been introduced to the mobile terminal to increase communication capacity per unit frequency. However, if MIMO antennas are put closely, a strong mutual coupling occurred. Moreover, CA which uses multiple frequencies is also utilized to improve communication speed. Therefore, reducing mutual coupling in multiple frequencies is required. In this paper, we propose a dual-band decoupling method by using a short stub and a branch element and confirmed that the proposed model performed decoupling, increased radiation efficiency.

key words: *MIMO, CA, decoupling, dual-band, short stub*

1. Introduction

Recently, also in a small wireless terminal such as a mobile phone, large capacity data for instance high definition movies and images are needed to communicate stable. For that, to increase channel capacity per frequency, MIMO (Multiple Input Multiple Output) technology [1] which uses multiple antennas are introduced to many wireless terminals. From the viewpoint of designability or convenience, miniaturization of wireless terminals is required. Hence, miniaturization of MIMO antennas is also required at the time of installing MIMO to small wireless terminals. If multiple antennas are put closely, the area of antennas can be reduced, and it leads to improvement in designability and miniaturization of wireless terminals. However, strong mutual coupling, which causes decreasing of radiation efficiency or channel capacity, occurs by putting multiple antennas in proximity [2].

In addition, CA (Carrier Aggregation) technology [3] which uses multiple frequencies is also installed to many mobile terminals. Thus, corresponding to CA, decoupling method for multiple frequencies is needed.

Many decoupling methods is proposed so far. First, inserting slit to GND plane has a problem with the limit of component placement in the GND plane by slit [4]. Furthermore, fixing EBG (Electromagnetic Band Gap) between antennas is also suggested, however, space for EBG structure is needed, and then, it's not suitable for miniaturization [5]. Thereby, we have considered as other decoupling methods, connecting between 2 element monopole antennas by wiring or circuit [6]–[9]. These methods have no limit of placing component and are just connecting between antennas by the circuit. Therefore, it is possible to take countermeasures to antenna part only.

In the previous study, the method of connecting antennas by susceptance circuit composed inductor L and capacitor C in parallel [10]. However, the wiring is required to connect the antenna via the lumped element (L or C), and the resistance of the lumped element causes power loss as well. Hence, the method of using an antenna shape of three elements with different length without lumped element is proposed instead of the susceptance circuit [11]–[13]. In this method, it is necessary to use the desired length element for the operation frequency. There is a problem of increasing antenna volume by the largest element in trifurcation elements. Thus, further miniaturization is required.

In this paper, branch element is regarded as an open stub, we propose the dual-band decoupling method of suppressing antenna volume by replacing the largest element in trifurcation elements with a short stub.

Section 2 explains the decoupling condition and the decoupling methods of connecting antennas by susceptance circuit or using trifurcation elements related to our research, then, we mention the problem of these methods. In Sect. 3, following problems in the previous studies, a proposed model with the short stub and the branch element and its Y-parameter are indicated. Section 4 shows S-parameter, current distribution, radiation efficiency, power losses, and radiation pattern, then, we confirm the effect of the decoupling by the proposed model. Section 5 is that proposed model is compared with previous methods of susceptance circuit and trifurcation. In addition, it is shown that the proposed method can be designed at nearly dual-frequencies. We conclude this study in Sect. 6.

2. Previous Decoupling Methods by Using Susceptance Circuit or Trifurcation Element

In this section, we introduce conventional the dual-band decoupling method by using susceptance circuit or trifurcation elements.

In this paper, we use 2 element monopole antennas assuming 2×2 MIMO with CA.

Decoupling condition is $Y_{21} = 0$ [9], and it is needed to make antenna admittance Y_{21} as close as possible to 0 S. For this reason, both $\mathrm{Re}(Y_{21})$ and $\mathrm{Im}(Y_{21})$ are set closely to 0 S.

In a previous study [10], due to the connection between

Manuscript received November 22, 2018.
Manuscript revised January 8, 2019.
Manuscript publicized February 20, 2019.

[†]The authors are with the Graduate School of Engineering and science, Chiba University, Chiba-shi, 263-8522 Japan.
[††]The author is with the Panasonic Corporation, Yokohama-shi, 224-0054 Japan.
a) E-mail: omei@m.ieice.org

DOI: 10.1587/transcom.2018EBP3340

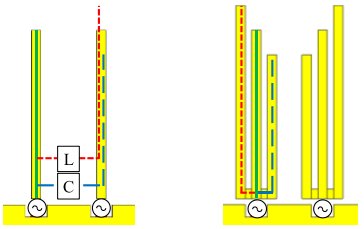

(a) Connected by L and C (b) Trifurcation element

Fig. 1 Current path of L or C and branch element.

antennas via susceptance circuit composed inductor L and capacitor C in parallel, dual-band decoupling method is realized.

In this method, 2 element monopole antennas are designed in order to resonance between two desired frequencies, first. Then, inserting a susceptance circuit which has the same value as $\mathrm{Im}(Y_{21})$ in desired two frequencies, $\mathrm{Im}(Y_{21}) = 0$ can be obtained. Regarding $\mathrm{Re}(Y_{21})$, we utilize an area of almost $\mathrm{Re}(Y_{21}) = 0$.

However, this method needs to connect antennas and insert L or C, thus, the wiring is required, and resistance included in L or C causes power loss.

Therefore, considering the characteristic of change the current path by L or C, method of trifurcation element is also proposed [11]–[13]. ([12] focus on proposing new decoupling method. However, reference [13] doesn't propose a novel decoupling method but mentions broadband for trifurcation decoupling. Reference [11] summarizes these articles.) Figure 1 shows equivalent current path length at the excitation of left feed port. If antennas are connected by L and C in parallel, there are three current paths; monopole at the left side and another monopole via L and C like Fig. 1(a). Furthermore, C shortens the current path, thus, decoupling equivalent to C connecting can be realized by adding a shorter branch element to the monopole. Similarly, decoupling equivalent to L connecting can be realized by adding a longer branch element. Hence, to perform equivalent decoupling, shorter and longer branch elements are added one each like Fig. 1(b). It is regarded as a trifurcation structure. This method can decouple at two frequencies without connection and without susceptance circuit between antennas like Fig. 1(a). However, the longer branch element is longer than the monopole, thus, there is a problem of increasing antenna volume for decoupling.

3. Proposing Dual Frequency Decoupling Method of Using a Branch Element and a Short Stub

Although there is an advantage that there is no connection between the antennas by a susceptance circuit as shown in Sect. 2, there remains a problem of an increase in antenna volume by longer branch element. Then, the longer branch element is miniaturized to dual-band decoupling in this paper.

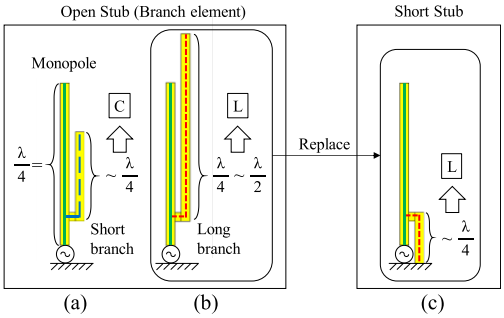

Fig. 2 Characteristics of an open stub and a short stub.

3.1 Replace the Longer Branch Element to the Short Stub

The branch element in Sect. 2 is regarded as an open stub because its tip opens. The decoupling concept figure using stubs is shown in Fig. 2 [14]. Replacing C between antennas with shorter branch element in Fig. 2(a), L with longer branch element in Fig. 2(b). Both (a) and (b) is regarded as adding the open stub to the monopole.

The length of the open stub needs less than $\lambda/4$ to exhibit capacitive, from $\lambda/4$ to $\lambda/2$ to exhibit inductivity. λ indicates effective wavelength considering wavelength shortening. This monopole antenna operates at about $\lambda/4$. Thus, to realize the decoupling equivalent to C connecting by the open stub, the length is less than the monopole ($\lambda/4$). Nevertheless, to realize the decoupling equivalent to L connecting by the open stub, the length needs more than the monopole ($\lambda/4$), then, this causes increasing antenna volume.

For this reason, the longer branch element (equivalent to L connecting) is changed to a short stub. The length of the short stub needs less than $\lambda/4$ to exhibit inductivity like Fig. 2(c). Hence, in the viewpoint of decreasing antenna volume, the short stub is more effective than the longer branch element in the decoupling equivalent to L connecting.

In reference [15], decoupling is performed only using the short stub at single frequency. Moreover, references [11]–[13] use only open stubs to decouple at dual-band.

Therefore, originality of this paper compared with [11]–[13] and [15] is that short stub is attached instead of a longer branch element in trifurcation model for miniaturization of the antenna and that both the short stub and the open stub are used for dual-band decoupling.

3.2 Proposed Model (Analysis Model)

Figure 3(a) shows the proposed dual-band decoupling model. Desired frequencies are 1.8 GHz and 2.1 GHz which are used same in CA. Models consist of one side copper plate FR-4 (Flame Retardant Type 4) substrate whose thickness is 0.8 mm and are symmetrical to the z-axis. GND plane size is 100×50 mm. 2 element monopole antennas whose length is 27.2 mm, width is 1.5 mm are arranged with interval 9.0 mm, and a branch element and a short stub are added in inside of the monopole. Feed point provides between antennas and

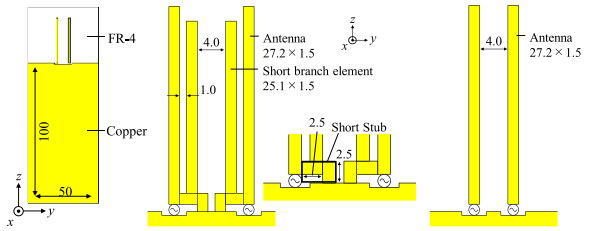

(a) Proposed model (b) Without decoupling model (only monopoles)

Fig. 3 Analysis antenna models (Unit: mm).

GND plane, the non-feeding point is terminated by 50 Ω. Port numbers are 1, 2 from the right side port. Constants of FR-4 are relative permittivity $\varepsilon_r = 4.3$, $\tan\delta = 0.01$, constants of copper are conductivity $\sigma = 5.8 \times 10^7$ S/m, permeability $\mu = 4\pi \times 10^{-7}$ H/m, we simulated by time domain solve of Micro Wave Studio by CST [16].

Figure 3(b) is without decoupling model to confirm the effects of the decoupling by the proposed model. In the proposed model, the nearest antenna distance is 4.0 mm (between short branches). Hence, we compare these models to be the same conditions which include antenna length and width of proposed model 27.2 mm, 1.5 mm and the nearest interval not 9.0 mm but 4.0 mm (between short branches). It is assumed the worst condition.

(a) S_{11} and (b) Y_{21} of only monopoles removing the branch element and the short stub of the proposed model shown in Fig. 4. From Fig. 4(a), the downtrend of S_{11} is obtained at around 1.9 GHz, the resonance of Y_{21} also generated at around the downtrend of S_{11} (1.9 GHz). The decoupling is performed at higher frequency 2.1 GHz than 1.9 GHz by the branch element, at lower frequency 1.8 GHz by the short stub.

The design method of branch element is shown in [17], short stub in [15] respectively. Figure 5 shows Y_{21} of the proposed model. First, the resonance of monopole is confirmed at 1.93 GHz. In addition, the resonance by the branch element appears at higher frequency 2.16 GHz, the resonance by the short stub appears at lower frequency 0 GHz (DC). According to [14] and [15], short branch let appear resonance at higher than monopole's resonance and short stub make the resonance at lower. In addition, this operation is the same as connecting antennas by L and C in parallel, hence, the branch element exhibits capacitive and the short stub exhibits inductivity.

Moreover, at 1.8 GHz and 2.1 GHz which are desired frequencies, $\mathrm{Im}(Y_{21})$ is 0 S (Fig. 5(a)). And $\mathrm{Re}(Y_{21})$ is 1.2 mS at 1.8 GHz, 1.2 mS at 2.1 GHz, it can be regarded as almost 0 S (Fig. 5(b)), as a result, we obtained $Y_{21} = 0$ at both frequencies.

Then, we mention about the limitation of working frequency bands. In proposed method, the desired two frequencies must be selected one by one from higher and lower frequency, respectively, from the resonance generated by the monopole antenna. This is the limitation. In this manuscript, according to Fig. 5, the resonance by monopole is appeared

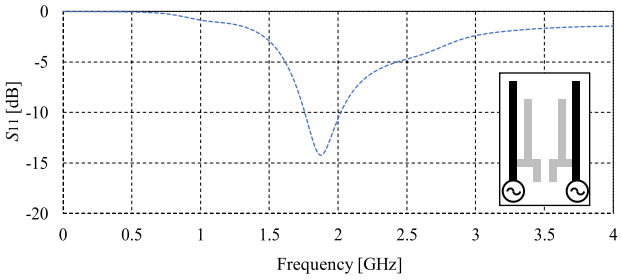

(a) S-parameter

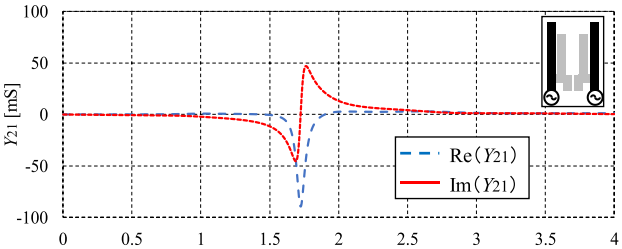

(b) Y-parameter

Fig. 4 S-parameter and Y-parameter of only antenna model.

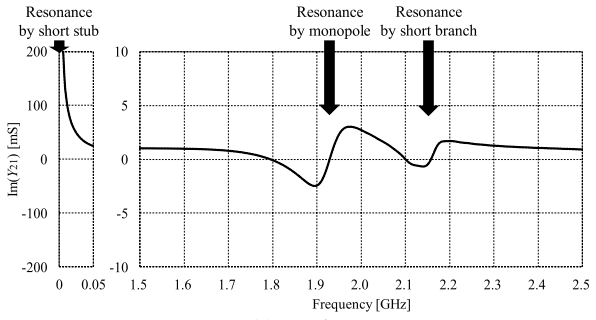

(a) Imaginary part

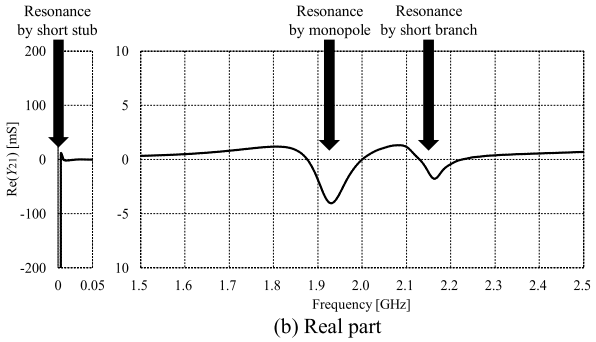

(b) Real part

Fig. 5 Y_{21} proposed model.

at 1.93 GHz, therefore, we chose two frequencies; 1.8 GHz where is lower and 2.1 GHz where is higher.

The proposed method tries to diminish the length of each element less than monopole length $\lambda/4$. According to a transmission line theory, the attached open stub which is shorter than $\lambda/4$ has C characteristic, generate the resonance higher frequency. Thus, decoupling at lower frequency than monopole's resonance is impossible. Similarly, if the short

stub which is shorter than $\lambda/4$ is added, exhibitivity, then the resonance is appeared at lower frequency (DC). Hence, it can't decouple at higher frequency resonance of monopole. From this reason, about desired two frequencies, limitation as mentioned above occurs.

4. Characteristics

4.1 S-Parameters

S-parameters of each model is shown in Fig. 6. Both models are using a matching circuit and obtain matching condition that S_{11} is about -10 dB at desired frequencies. Moreover, good agreement between simulated value shown in lines and the measured value shown in markers is confirmed, thus, the validity of simulated value is indicated.

In without decoupling model Fig. 6(a), S_{21} is -3.4 dB at 1.8 GHz, -4.9 dB at 2.1 GHz which are strong mutual coupling. By contrast, in proposed model Fig. 6(b), S_{21} is -10.2 dB at 1.8 GHz, -15.5 dB at 2.1 GHz, hence, the mutual coupling reduced 6.8 dB, 10.6 dB, respectively.

4.2 Current Distribution

In Fig. 7 shows the current distribution of instantaneous value in case of exciting 1 W, 1.8 GHz sine wave from Port1. Port2 is terminated by 50 Ω. Figure 7(a) shows without decoupling model, Fig. 7(b) shows the proposed model. Figure 8 shows the current distribution at 2.1 GHz. (a) and (b) show the same models in Fig. 7.

Without decoupling model (Fig. 7(a) and Fig. 8(a)), current is concentrated at Port2 terminated by 50 Ω, therefore, the strong mutual coupling is confirmed according to the current distribution. On the other hand, in the proposed model (Fig. 7(b) and Fig. 8(b)), flowing current to Port2 decreases and reducing mutual coupling is confirmed by decoupling. Moreover, the current distributes monopole and the short stub strongly in Fig. 7(b), therefore, the decoupling at 1.8 GHz is performed by these. By contrast, at 2.1 GHz, the current distributes monopole and the branch element strongly in Fig. 8(b), thus, the decoupling is realized by these.

4.3 Radiation Efficiency and Power Loss

Conceptional diagram of radiation and power loss is shown in Fig. 9. P_r is radiation power, P_d is a coupling loss which we try to reduce, P_m is reflection loss at excitation port, P_Ω is a loss by the resistance of lumped element for matching circuit, P_{die} is a dielectric loss, P_{con} is a conductor loss.

Table 1 shows radiation power and various power losses at 1.8 GHz, Table 2 shows at 2.1 GHz similarly. Input power is 1 W. At 1.8 GHz, it is confirmed that coupling loss P_d is reduced from 0.46 W to 0.10 W and radiation power is improved from -4.4 dB to -2.0 dB. Also at 2.1 GHz, P_d

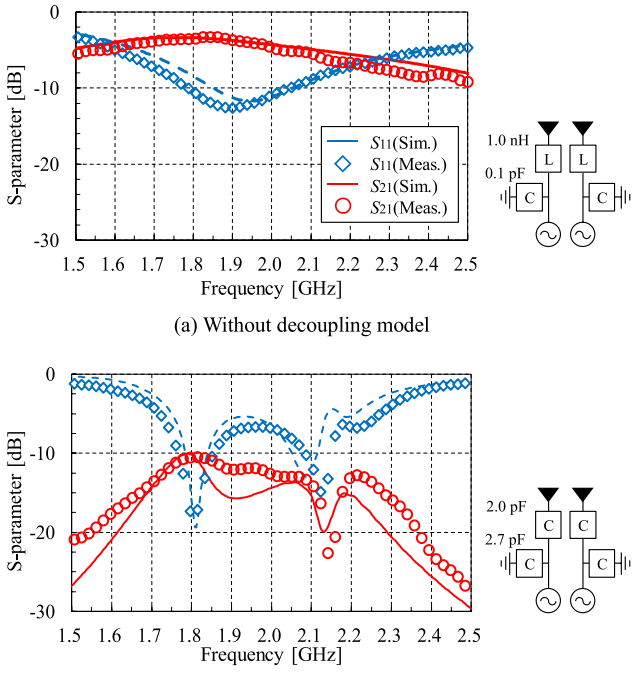

(a) Without decoupling model

(b) Proposed model

Fig. 6 S-Parameters with matching circuit.

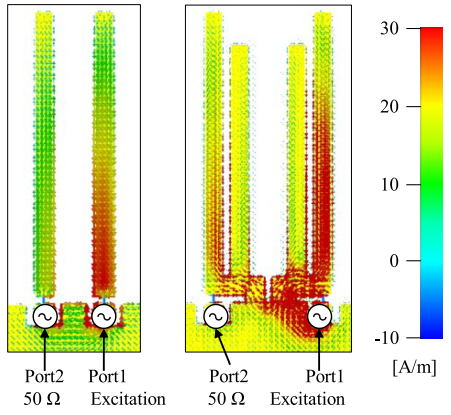

(a) Without decoupling model (b) Proposed model

Fig. 7 Current distribution at 1.8 GHz.

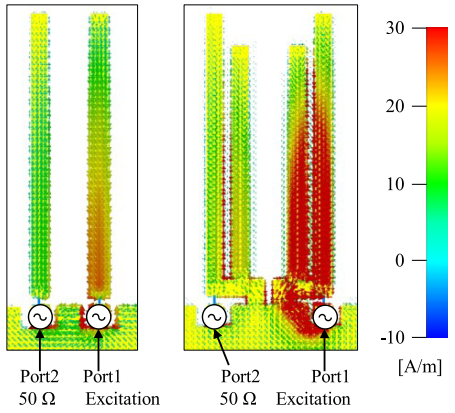

(a) Without decoupling model (b) Proposed model

Fig. 8 Current distribution at 2.1 GHz.

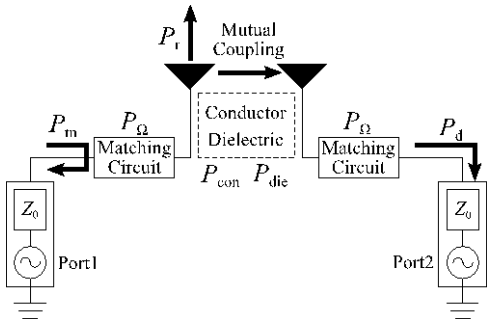

Fig. 9 Conceptional diagram of radiation and power loss.

Table 1 Radiation efficiency and each of power loss at 1.8 GHz.

Input Power = 1 W	Without decoupling	Proposed
Radiation efficiency	-4.4 dB (0.36)	-2.0 dB (0.63)
Coupling loss	0.46	0.10
Reflection loss	0.14	0.04
Matching circuit loss	0.03	0.12
Dielectric loss	0.01	0.10
Conductor loss	0.00	0.00

Table 2 Radiation efficiency and each of power loss at 2.1 GHz.

Input Power = 1 W	Without decoupling	Proposed
Radiation efficiency	-2.8 dB (0.52)	-2.0 dB (0.63)
Coupling loss	0.32	0.05
Reflection loss	0.12	0.05
Matching circuit loss	0.03	0.15
Dielectric loss	0.01	0.12
Conductor loss	0.00	0.00

is reduced from 0.32 W to 0.05 W and radiation power is improved from −2.8 dB to −2.0 dB.

However, in the proposed model, the large power loss of dielectric and matching circuit is confirmed at both frequencies. According to Fig. 7 and Fig. 8, current flows more strongly than without decoupling model at both frequencies. Hence, dielectric loss is large. Low loss dielectric substrate whose tan δ is less than 0.005 [18] is developed, hence, dielectric loss can be reduced by using it. Lumped elements with the resistance are used for the matching circuit. By the decoupling, antenna impedance is changed, then, the matching circuit loss became large by the arrangement of the matching circuit. Matching circuit loss can be reduced by using low resistance lumped element.

Moreover, conductor loss is zero in Table 1 and Table 2 in both models. Nevertheless, conductor loss is not zero in fact. However, its value is too low. We round off to the third decimal place, therefore, we have no choice but to list conductor loss as 0 W.

4.4 Radiation Pattern

Figure 10 shows a radiation pattern of xy-plane at 1.8 GHz. (a) is without decoupling model, (b) is proposed model. Good agreement between simulated value shown in lines and

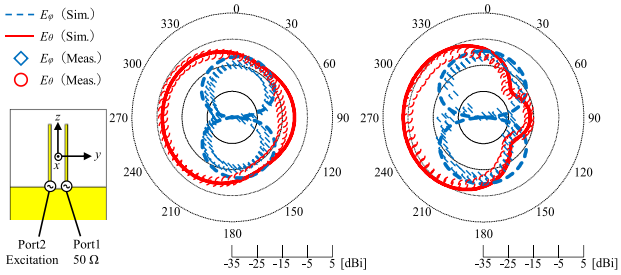

(a) Without decoupling model (b) Proposed model

Fig. 10 Radiation pattern of xy-plane at 1.8 GHz.

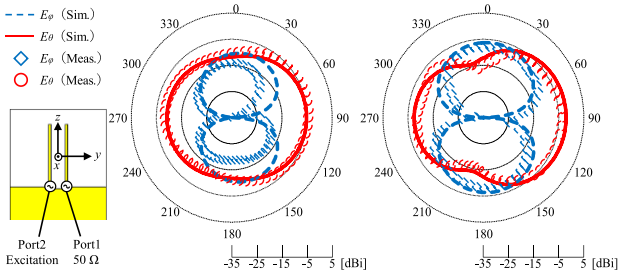

(a) Without decoupling model (b) Proposed model

Fig. 11 Radiation pattern of xy-plane at 2.1 GHz.

the measured value shown in markers is confirmed, therefore, the validity of simulated value is indicated. In Fig. 10, a gain of the proposed model's E_θ which is the main polarization is around 4.1 dBi higher than without decoupling model in the -y-direction (φ = 270 deg.). At 2.1 GHz shown in Fig. 11, E_θ is around 3.1 dBi higher than without decoupling model in the y-direction (φ = 90 deg.).

As a result, improving gain is confirmed at both frequencies.

5. Comparing with Other Previous Methods

In this section, the proposed model is compared with the susceptance circuit method [10] and trifurcation method [11], [12]. Antenna models of these previous studies are shown in Fig. 12. Desired frequencies are 1.5 GHz and 2.5 GHz in the method of the susceptance circuit, 1.5 GHz and 2.0 GHz in the method of the trifurcation method.

5.1 Coupling Loss and Radiation Efficiency

Table 3 shows coupling loss (Input power: 1 W) and Table 4 shows radiation efficiency (Input power: 1 W) of three methods at desired frequencies. These three models are different from element length, antenna interval, and element width. Therefore, this comparing is not strict but simple. The coupling loss of proposed method at lower desired frequency is larger than other two method at lower desired frequency because current flows to other port via short stub from Fig. 7(b). Additionally, at higher desired frequency, the coupling loss of proposed method is the smallest slightly of the three methods. In radiation efficiency, proposed method

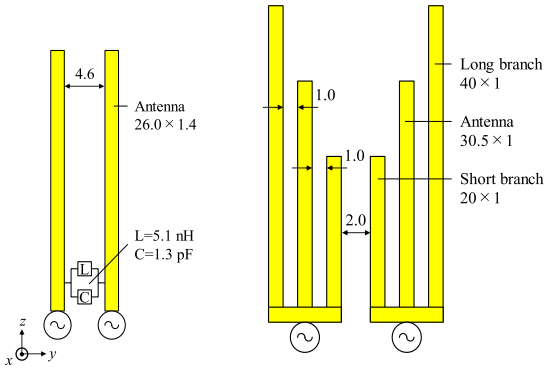

(a) With susceptance circuit [10] (b) Trifurcation Elements [11-12]

Fig. 12 Antenna models of previous studies.

Table 3 Coupling loss of each method (Input power = 1 W).

Susceptance circuit		Trifurcation element		Proposed method	
1.5 GHz	2.5 GHz	1.5 GHz	2.0 GHz	1.8 GHz	2.1 GHz
0.01 W	0.06 W	0.03 W	0.07 W	0.10 W	0.05 W

Table 4 Radiation efficiency of each method (Input power = 1 W).

Susceptance circuit		Trifurcation element		Proposed method	
1.5 GHz	2.5 GHz	1.5 GHz	2.0 GHz	1.8 GHz	2.1 GHz
0.41 W	0.70 W	0.60 W	0.68 W	0.63 W	0.63 W

Table 5 The value of L and C in Fig. 13.

f_{dl} [GHz]	f_{dh} [GHz]	L [nH]	C [pF]
1.5	2.5	2.9	4.3
	2.4	3.3	2.8
	2.3	4.2	2.0
	2.2	4.9	1.6
	2.1	5.5	1.3

is better efficiency than other two method at lower desired frequency. However, at higher desired frequency, proposed method is the worst. We considered that the dielectric loss has increased due to flowing strong current to branch element according to Fig. 8(b) and Table 2.

5.2 The Closest Designable Frequency Interval (CDFI)

The proposed method can decouple while desired frequencies are apart 0.3 GHz (Desired frequencies are 1.8 GHz and 2.1 GHz). Hence, the closest designable frequency interval (CDFI) of this method is 0.3 GHz. In the case of other previous methods, we verify whether the CDFI is close 0.3 GHz.

Figure 13 shows $\mathrm{Im}(Y_{21})$ of Fig. 12(a) model while one decoupling frequency is fixed at 1.5 GHz ($= f_{dl}$), the other changes lower from 2.5 GHz by 0.1 GHz ($= f_{dh}$). The value of L and C is put on Table 5.

From this result, $\mathrm{Im}(Y_{21}) = 0$ is approximately obtained at both desired frequencies until $f_{\mathrm{dh}} = 2.3$ GHz. However, in $f_{\mathrm{dh}} = 2.2$ GHz, although the resonance appears, $\mathrm{Im}(Y_{21}) = 0$ can't be obtained, having a positive value. Hence, decoupling condition isn't satisfied. At $f_{\mathrm{dh}} = 2.1$ GHz, the highest resonance disappears and fixed f_{dl} is different from 1.5 GHz. Therefore, the CDFI of the method of susceptance circuit is 0.8 GHz.

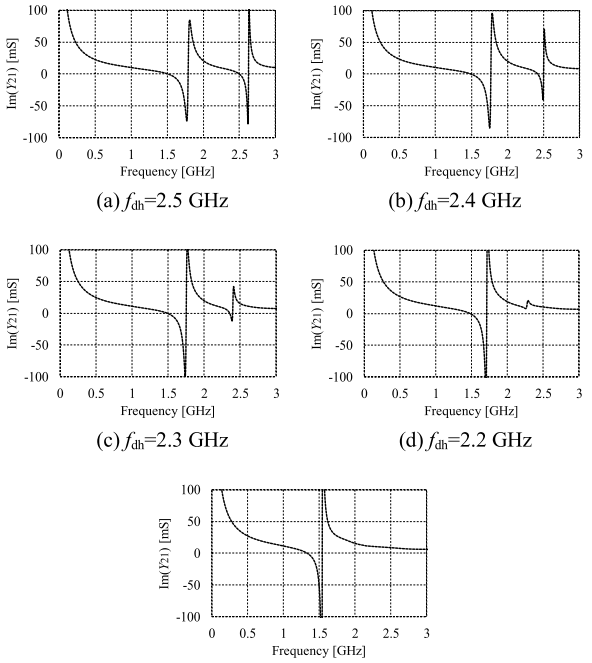

(a) f_{dh}=2.5 GHz (b) f_{dh}=2.4 GHz

(c) f_{dh}=2.3 GHz (d) f_{dh}=2.2 GHz

(e) f_{dh}=2.1 GHz

Fig. 13 $\mathrm{Im}(Y_{21})$ of changed f_{dh} lower by 0.1 GHz, f_{dl}=1.5 GHz fixed.

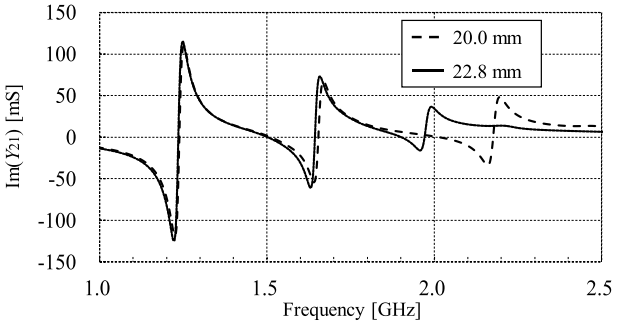

Fig. 14 $\mathrm{Im}(Y_{21})$ when the short branch element is 20.0 or 22.8 mm.

Figure 14 shows $\mathrm{Im}(Y_{21})$ when the length of the short branch is 20.0 mm or 22.8 mm while the length of long branch and the antenna is fixed in trifurcation model Fig. 12(b).

According to Fig. 14, lower decoupling frequency (f_{dl}) is not changed, and f_{dh} is 2.0 GHz if the length of the short branch is 20.0 mm, f_{dh} is 1.9 GHz if the length of the short branch is 22.8 mm.

Figure 15 shows $\mathrm{Im}(Y_{21})$ the length of the short branch is altered from 24.0 mm to 25.0 mm by 0.2 mm. Other element length is fixed the same as the last time.

From Fig. 15, the longer the short branch is, the lower f_{dh} (higher decoupling frequency) moves. Until the short branch length is 24.4 mm, $\mathrm{Im}(Y_{21}) = 0$ is obtained, how-

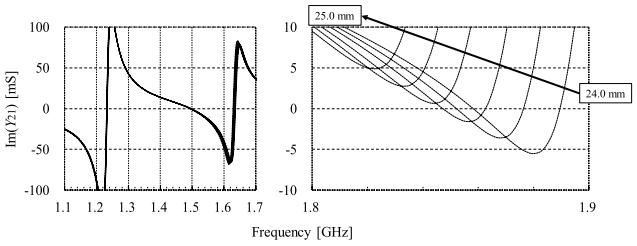

Fig. 15 Im(Y_{21}) of changed the short branch element from 24.0 mm to 25.0 mm by 0.2 mm.

ever, since 24.6 mm, decoupling condition isn't satisfied and $\mathrm{Im}(Y_{21}) = 0$ can't be get at 1.8 GHz. This method is also, decoupling where desired frequencies are close 0.3 GHz can't perform. Therefore, the superiority of the proposed model in the design of close frequencies is proved.

We consider this reason as follows. From Fig. 15 right, f_{dh} moves lower since the frequency of resonance by the short branch moves lower as the short branch becomes longer. However, the entire resonance of the short branch has positive value, then $Y_{21} = 0$ can't be obtained. The positive value of Y_{21} (admittance) indicates capacitive (C characteristic), it is considered that the capacity between port1 and 2 occurs mainly by between the long branches or other branch. In the proposed method, because the long branch is replaced by the short stub, the capacity between antennas is reduced. As a result, f_{dh} can be made lower frequency and the CDFI of the proposed method is the narrowest compared with the other methods is conceived.

Additionally, in reference [10] and [11], [12], S_{21} at desired frequencies are low, however, high coupling is observed in other frequency bands. On the other hand, proposed model is able to reduce mutual coupling in wide band with peak at −10.2 dB at 1.8 GHz. In terms of the fractional bandwidth of S_{21}, proposed model is effective.

6. Conclusion

In this paper, we proposed the dual-band decoupling method by using the short stub and the branch element equivalent to the trifurcation method. Desired frequencies are set to 1.8 GHz and 2.1 GHz, as a result of adding the short stub and shorter branch elements to 2 element monopole antennas which are assuming 2×2 MIMO communications, mutual coupling S_{21} is lower 6.8 dB at 1.8 GHz, 10.6 dB at 2.1 GHz, and the radiation efficiency is improved by 2.4 dB at 1.8 GHz and 0.8 dB at 2.1 GHz. Hence, it is confirmed that the decoupling by using the short stub and the branch element can be performed at presented closely dual frequencies this time. In addition, as a result of comparing other previous methods, the ability of reducing coupling loss and improving radiation efficiency is same at these, and only proposed can design under the condition of decoupling frequencies are close 0.3 GHz.

To increase the bandwidth in the proposed model and to propose the decoupling method corresponding to more than 3 element MIMO are future studies.

References

[1] A.J. Paulraj, D.A. Gore, R.U. Nabar, and H. Bolcskei, "An overview of MIMO communications-A key to gibabit wireless," Proc. IEEE, vol.92, no.2, pp.198–218, Feb. 2004.
[2] Y. Karasawa, "MIMO propagation channel modeling," IEICE Trans. Commun. (Japanese Edition), vol.J86-B, no.9, pp.1706–1720, Sept. 2003.
[3] J. Wannstrom, "LTE-advanced," Third Generation Partnership Project (3GPP), 2012.
[4] T. Ohishi, N. Odachi, S. Sekine, and H. Shoki, "Low pattern correlation and low mutual coupling diversity antenna with a slit," IEICE Trans. Commun. (Japanese Edition), vol.J90-B, no.9, pp.844–853, Sept. 2007.
[5] J. Itoh, N. Michishita, and H. Morishita, "A study of the mutual coupling reduction between two inverted-F antennas using mushroom-type EBG structures," IEICE Technical Report, AP2007-122, Jan. 2008.
[6] J. Kim, M. Han, C. Lee, and J. Choi, "Dual band MIMO antenna using a decoupling network for WLAN application," ICACT 2011, pp.624–627, Feb. 2011.
[7] M.M. Albannay, J.C. Coetzee, X. Tang, and K. Mouthaan, "Dual-frequency decoupling for two distinct antennas," IEEE Antennas Wireless Propag. Lett., vol.11, pp.1315–1318, Oct. 2012.
[8] L. Zhao and K.L. Wu, "A dual-band coupled resonator decoupling network for two coupled antennas," IEEE Trans. Antennas Propag., vol.63, no.7, pp.2843–2850, July 2015.
[9] S. Chen, Y. Wang, and S. Chung, "A decoupling technique for increasing the port isolation between two strongly coupled antennas," IEEE Trans. Antennas Propag., vol.56, no.12, pp.3650–3658, Dec. 2008.
[10] H. Sato, Y. Koyanagi, K. Ogawa, and M. Takahashi, "A method of dual-frequency decoupling for closely spaced two small antennas," IEICE Trans. Commun. (Japanese Edition), vol.J94-B, no.9, pp.1104–1113, Sept. 2011.
[11] K. Kuriyama, H. Sato, and M. Takahashi, "A decoupling method for MIMO antenna using trifurcation elements," IEICE Communication Express, vol.6, no.6, pp.298–303, Jan. 2017.
[12] K. Kuriyama, K. Okuda, and M. Takahashi, "Dual-band decoupling method for two MIMO antenna using trifurcation elements," 2016 IEEE International Symposium on Antennas and Propagation (APSURSI), pp.2199–2200, Fajardo, 2016.
[13] K. Kuriyama, H. Sato and M. Takahashi, "Broadband characteristic of dual-band decoupling for closely spaced antennas," 2016 International Symposium on Antennas and Propagation (ISAP), pp.148–149, Okinawa, 2016.
[14] H. Nebiya and K. Uetake, "Ubiquitous musen kougaku to bisai RFID-musen IC tag no gijutsu (Ubiquitous wireless engineering and micro RFID-wireless IC tag technology)," Tokyo denki daigaku syuppankyoku, second edition, April 2004.
[15] T. Miyasaka, H. Sato, and M. Takahashi, "A decoupling method for 2 elements MIMO antennas using a short stub," IEICE Communication Express, 2018XBL0093, vol.7, no.10, pp.364–368, 2018.
[16] CST STUDIO SUITE 2017, http://www.cst.com
[17] H. Sato, Y. Koyanagi, K. Ogawa, and M. Takahashi, "A decoupling method for MIMO antenna arrays using branch shape elements," IEICE Communication Express, vol.3, no.11, pp.330–334, Nov. 2014.
[18] T. Nozawa, "5G de teisonshitsu yudentaikiban ga omotebutai ni, FR-y ya polyimide wo daitai (Low loss substrate is the front stage in 5G, replacing FR-4 and polyimide)," Nikkei Electronics, pp.45–50, Aug. 2017.

Takuya Miyasaka was born in Nagano, Japan in 1994. He received the B.E. degree from Chiba university, Japan in 2017. He is currently pursuing the M.E. course at Chiba university, engaging in the research on Antenna engineering.

Hiroshi Sato was born in Tokyo, Japan, on August 2, 1975. He received B.S. and M.S. degree in electrical engineering from Tokyo City University, Japan, in 1998 and 2000, and Ph.D. degree in electrical engineering from Chiba University, Japan, in 2015. From 2004 to 2012, he has been with Panasonic Mobile Communication Co., Ltd., Yokosuka, Japan. And is currently a leader of the R&D project for mobile phone antennas in Panasonic Corporation, Yokohama, Japan. His research interests include small antenna, MIMO antenna and decoupling technique. He was the recipient of the Best Paper Award from the Institute of Electronics, Information and Communication Engineers (IEICE) Transactions of Japan in 2012. He is a member of IEICE and IEEE.

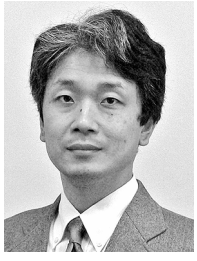

Masaharu Takahashi was born in Chiba, Japan in December 1965. He received the B.E. degree in electrical engineering from Tohoku university, Miyagi, Japan in 1989, and the M.E. and D.E. degrees in electrical engineering from the Tokyo Institute of Technology, Tokyo Japan, in 1991 and 1994, respectively. From 1994 to 1996, he was a Research Associate, and from 1996 to 2000, an Assistant Professor with the Musashi Institute of Technology, Tokyo, Japan. From 2000 to 2004, he was an Associate Professor with the Tokyo University of Agriculture and Technology, Tokyo, Japan. He is currently an Associate Professor with the Research Center for Frontier Medical Engineering, Chiba University, Chiba, Japan. His main interests are electrically small antennas, planar antennas, and EM compatibility. He was the recipient of the 1994 IEEE Antennas and Propagation Society (IEEE AP-S) Tokyo Chapter Young Engineer Award.